ELSEVIER

Biophysical Chemistry 105 (2003) 391–409

Biophysical Chemistry

www.elsevier.com/locate/bpc

Molecular and mesoscale structures in hydrophobically driven aqueous solutions

J.L. Finney[a,*], D.T. Bowron[b], R.M. Daniel[c], P.A. Timmins[d], M.A. Roberts[e]

[a]*Department of Physics and Astronomy, University College London, London, UK*
[b]*ISIS Facility, Rutherford Appleton Laboratory, UK*
[c]*Department of Biological Sciences, University of Waikato, New Zealand*
[d]*Institut Laue-Langevin, Grenoble, France*
[e]*Daresbury Laboratory, UK*

Received 30 September 2002; received in revised form 10 December 2002; accepted 10 December 2002

Abstract

Since Kauzmann's seminal 1959 paper, the hydrophobic interaction has dominated thinking on the forces that control protein folding and stability. Despite its wide importance in chemistry and biology, our understanding of this interaction at the molecular level remains poor, with little experimental evidence to support the idea of water ordering close to a non-polar group that is at the centre of the standard model for the source of the entropic driving force. Developments over recent years in neutron techniques now enable us to see directly how a non-polar group actually affects the molecular structure of the water in its immediate neighbourhood. On the basis of such work on aqueous solutions of small alcohols, the generally accepted standard model is found to be wanting, and alternative sources of the entropic driving force are suggested. Moreover, the fact that we can now follow changes in hydrogen bonding as the alcohol concentration is varied gives us the possibility of explaining the concentration dependence of the enthalpy of mixing. Complementary studies of solute association on the mesoscopic scale show a rich concentration and temperature behaviour, which reflects a complex balance of polar and non-polar interactions. Unravelling the detailed nature of this balance in simple aqueous amphiphiles may lead to a better understanding of the forces that control biomolecular structural stability and interactions.
© 2003 Elsevier Science B.V. All rights reserved.

Keywords: Non-polar interactions; Aqueous solution structure; Entropic driving force; Solution structure; Protein stability; Hydrophobic interaction

1. Introduction

Following Walter Kauzmann's seminal 1959 paper [1] on the forces relevant to protein denaturation, the hydrophobic interaction has dominated much of the thinking of the last 50 years concerning biomolecular interactions in solution. Most researchers in biochemistry and structural biology will assert that the hydrophobic interaction is the dominant interaction in driving the folding and association of proteins. Moreover, it is central

*Corresponding author. Tel.: +44-20-7679-7850; fax: +44-20-7969-1360.
E-mail address: j.finney@ucl.ac.uk (J.L. Finney).

0301-4622/03/$ - see front matter © 2003 Elsevier Science B.V. All rights reserved.
doi:10.1016/S0301-4622(03)00104-2

to many self assembly processes, and is clearly relevant to the maintenance of lipid bilayers and related biological entities such as cell membranes. Although the relative importance of the different kinds of interactions in processes such as protein folding continues to be controversial, the hydrophobic interaction clearly is of significant importance in the interactions in aqueous solutions of molecules containing non-polar moieties.

Despite its importance, what is happening at the molecular level when two non-polar groups interact in water remains unclear. In contrast, the thermodynamics of the association process is well established; when two non-polar groups come together in aqueous solution, the free energy change is negative. The enthalpic contribution to the process can be either positive or negative, depending on the system. The central point, however, is that the entropic change is positive, and that this term dominates the free energy change. The process is entropy driven.

What is the source of the entropic driving force? The 'standard' model stems from the classical 1945 paper of Frank and Evans [2]. Briefly, it argues that the entropic contribution relates to changes in the structure of the solvent in the environment of the non-polar group. On dissolving the solute in water, the hydration shell of the non-polar group is thought to have a structure that is 'more ordered' than that of water in the bulk. Thus, when two such groups come together in aqueous solution, some of the water in the two displaced hydration shells is expelled to the bulk with a consequent gain in entropy of the system. It is this change in entropy of the *solvent* which is considered to be the entropic driving force of the hydrophobic association process.

What is the nature of this solvent 'ordering'? As we are already dealing with a liquid, we have somehow to quantify this ordering not only with respect to a structure that is highly disordered, but also with respect to a reference state (bulk water) that itself is unfamiliar to most workers. Frank and Evans [2] talked of the non-polar molecule modifying 'the water structure in the direction of greater 'crystallinity'—the water, so to speak, builds a microscopic iceberg around it'. This use of terminology—the 'iceberg'—has entered the collective unconscious. Frank and Evans used this term 'to represent a microscopic region … in which water molecules are tied together in some sort of quasi-solid structure', though they emphasised that they did not imply 'that the structure is exactly ice-like'. Today also, few would think of the 'iceberg' as crystalline ordering of the water molecules as in ice. The general picture seems to be that the hydration structure (the 'iceberg') relates to that of the clathrate cage structures found in gas hydrates [3,4]. An example of one of these cages is shown in Fig. 1. The presence of 5-fold ring structures is a natural consequence of the way in which even spheres maximise their packing around a sphere, and we should note in passing that such 5-fold ring structures are a major constituent in the structure of bulk water itself. So the accepted view is that the hydration water of a non-polar group is similar to that in typical gas hydrates, and that this water is 'more ordered' than it is in the bulk. Bringing together two such groups in solution will break up this structure as the water molecules in the hydration shell are expelled to the bulk. Hence the entropic gain.

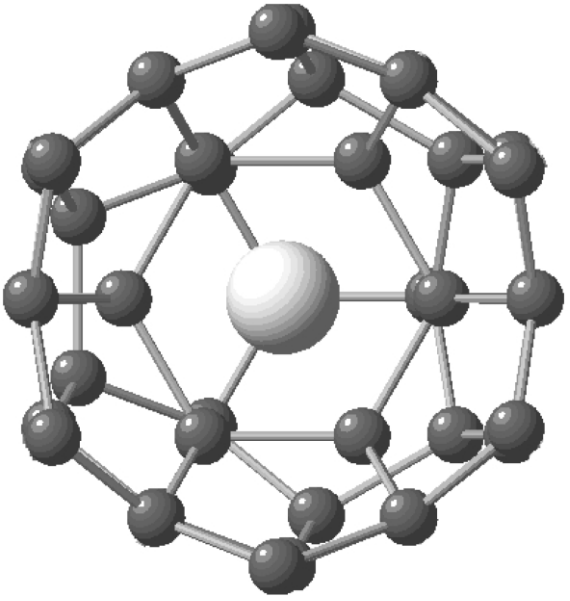

Fig. 1. A clathrate cage containing a guest molecule. The one shown here is the large cage of the type II clathrate.

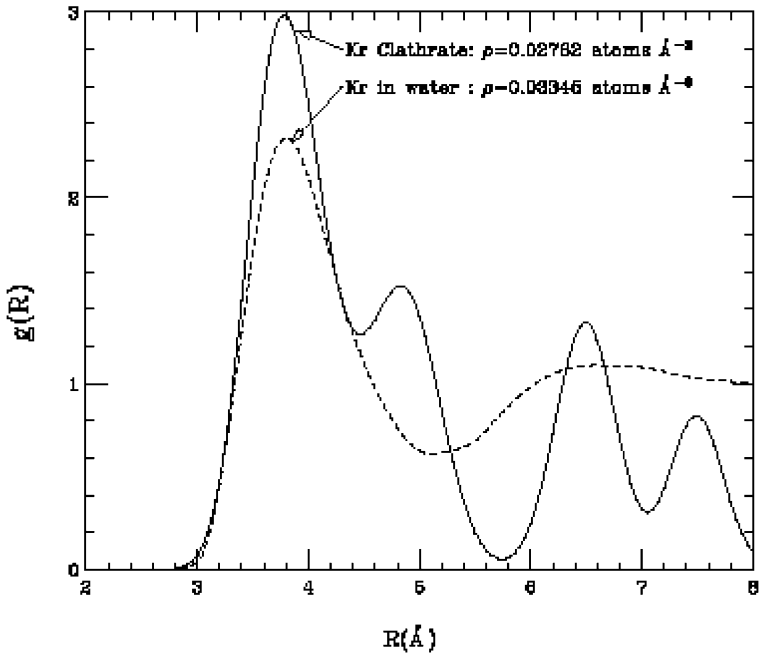

Fig. 2. Refined Kr–O partial rdf derived from the liquid state EXAFS spectrum at 5 °C and 110 bars, and the comparable function determined from the solid crystal data.

Although this 'water ordering' explanation is the currently accepted view, when we look for experimental justification, we are struggling. This is not surprising, as in order to provide experimental evidence of structural ordering, we need to determine the water structure in the hydration shell of a non-polar group. Measuring liquid structures themselves is difficult enough; obtaining information on the structure of that part of the water that is next to the non-polar group is an even taller order.

Perhaps the earliest attempt to obtain this information was X-ray scattering measurements of Folzer and Jeffrey on aqueous trimethylamine solutions in the early 1970s [5]. Even at the relatively high ~10% solute concentration used in those earlier measurements, a concentration at which essentially all the water should be hydration water, their modelling of the experimental data was unable to distinguish between a structural model based on the existence of clathrate-like hydration shells or the one that was used to fit earlier X-ray data of the pure liquid. They were thus unable to draw any conclusions about the nature of the expected water ordering they were looking for.

Things have moved on since then. With advances in the last decade in neutron scattering techniques, allied with computational developments to assist interpretation, we can now obtain detailed structural information on solutions, and so test the standard model. We discuss here the results of a number of experiments on appropriate aqueous solutions of model systems which lead to structural information on the solvent at the molecular level. We find that not only is the standard model wanting, but that the experiments themselves suggest other sources for the entropic driving force that may be simpler than the current standard model. Finally, we present some new recent results on the temperature and concentration dependence of the structural behaviour at the mesoscopic level of aqueous amphiphile solutions in relation to the possible relevance of the hydrophobic interaction to the stability of thermophilic proteins.

2. Methods

2.1. What is a liquid structure?

The structure of a single component liquid is described by the radial distribution function $g(r)$ (the rdf), which quantifies the ratio between the local density of atoms at a distance r from an atom at the origin to the average number density ρ of atoms in the system. A diffraction experiment uses the known wavelength of the (usually X-ray or neutron) scattering probe to obtain the information on pair distance distributions that is contained in the radial distribution function. The scattering experiment measures the intensity scattered as a function of the scattering vector **Q**, defined simply as the difference between the scattered and incident wave vectors, with a magnitude $|\mathbf{Q}| = 4\pi \sin\theta/\lambda$, where 2θ is the scattering angle and λ the wavelength of the radiation used. From the scattered intensity, the structurally significant structure factor $S(Q)$ can be extracted which can then be related to the radial distribution function through a Fourier transform relationship:

$$[S(Q)-1] = 4\pi\rho \int_0^\infty r^2 \, dr[g(r)-1]\frac{\sin(Qr)}{Qr}. \quad (1)$$

This formalism is simply extended to deal with solutions. Consider a two component system, with components α and β, with N_α, N_β (where $N_\alpha + N_\beta = N$) atoms of each, and the atomic fractions of each component defined as $c_\alpha = N_\alpha/N$, $c_\beta = N_\beta/N$. The structure factor can be split into three terms – partial structure factors $S_{\alpha\beta}$ – each relating to different pairs of interacting atoms $\alpha\alpha$, $\beta\beta$ and $\alpha\beta$. Thus, a partial radial distribution function $g_{\alpha\beta}(r)$ is defined similarly to the radial distribution function, but with the added identification of the type of atom both at the local origin and at the distance r. We can then rewrite Eq. (1) as

$$[S_{\alpha\beta}(Q)-1] = 4\pi\rho \int_0^\infty r^2 \, dr[g_{\alpha\beta}(r)-1]\frac{\sin(Qr)}{Qr}. \quad (2)$$

For a two component system, we require 3 partial radial distribution functions $g_{\alpha\alpha}(r)$, $g_{\alpha\beta}(r)$, $g_{\beta\beta}(r)$ to describe the structure of the system. For an n component system, $n(n+1)/2$ partials are needed for a full structural description of the system. Each of these partial rdfs will be related to a partial structure factor that is embedded in the measured diffraction data, and taken together comprise the total structure factor

$$F(Q) = \sum_{\alpha,\beta} (2-\delta_{\alpha\beta}) b_\alpha b_\beta c_\alpha c_\beta [S_{\alpha\beta}(Q)-1] \quad (3)$$

where b_β, b_β are the scattering lengths of the components α and β.

2.2. Experimental determination of solution structures

A single diffraction experiment gives us access to only the total radial distribution function $g(r)$, which is a weighted sum of the partial rdfs. This is not very useful information for a solution: we need to get closer to determining the *partial* structure factors. The key to achieve this is given in Eq. (3): the fact that the total structure factor is a weighted sum gives us the way forward. One of the weighting factors is the scattering length of each component. If we could perform an experiment on the same system, but somehow change the scattering length b, we could perform more than one experiment on chemically similar systems, and begin to extract the kind of more detailed information we really want.

That we can indeed do this is made possible by the fact that the neutron is scattered by the nucleus, and many elements have different isotopic forms. If these isotopic forms had different neutron scattering lengths, then we could perform an additional experiment on a system in which we change only the isotope of one of the components. Referring to Eq. (3), we could then obtain from a second scattering experiment a different structure factor $F'(Q)$ in which, say b_α, is replaced by $b_{\alpha'}$. Now performing a third experiment replacing the isotope of the second component, b_β is replaced by $b_{\beta'}$. Alternatively, isotope α could be replaced by either a third isotope α'' (or what is in effect the same, a mixture of isotopes α and α'). We now would

have three equations with the three partial structure factors as the three unknowns. In principle these could be solved for, and the corresponding partial radial distribution functions obtained.

For relatively simple two component liquids and glasses, such 'full' partial structure factors—and hence 'full' partial radial distribution functions—have been extracted (see for example Ref. [6]). For the relatively complex systems in which we are interested here, performing the much larger number of isotopically distinct scattering experiments that would be necessary to extract all the partial rdfs looks a tall order. In the case of *t*-butanol in water—one of the systems we will consider below—there are 7 chemically distinct atoms in the system (methyl carbon, methyl hydrogen, central carbon, alcohol oxygen, alcohol hydroxyl hydrogen, water oxygen, water hydrogen). We would require $7\times 8/2=28$ isotopically distinct experiments to yield the 28 partial radial distribution functions (or 'partials' for short). Setting aside whether an appropriate set of isotopically distinct solutions could be prepared (not all elements have isotopes with significantly different scattering lengths), the requirements for neutron beam time—which is not cheap—would be extremely high. As we shall see below, there are other ways round the problem that enable us to obtain not only all the partials for a system such as this, but even to go beyond the partials to obtain even more detailed structural information on relatively complex solutions.

2.3. An example: t-butanol in water

For the *t*-butanol-water system, performing 28 isotopically distinct diffraction experiments is not a realistic possibility. The 'best' kind of isotopic substitution we can do on this system is to deuterate the hydrogens on (a) the methyl groups of the alcohol head group and (b) the water. In fact, for each substitution, we work with (a) fully deuterated; (b) fully hydrogenated; (c) a 50:50 hydrogen/deuterium mixture. This gives three values of the neutron scattering length of the substituted sites, and hence, for each triplet of substitutions, enables us to obtain three sets of (partial) radial distribution functions. We will call these $g_{HH}(r)$, $g_{HX}(r)$ and $g_{XX}(r)$. Here the subscript *H* refers to a site whose hydrogens are substituted, while the *X* subscript refers to all the non-substituted sites. Thus, for a set of substitutions on the methyl hydrogen sites of *t*-butanol, *H* refers to all the substituted methyl hydrogen sites, while *X* refers to all other sites.

The corresponding set of experiments can now be specified as follows:

1. Solvent–solvent distribution functions are probed through substitution on the water hydrogen sites to yield the (partial) radial distribution functions $g_{HH}(r)$, $g_{HX}(r)$ and $g_{XX}(r)$ for the solvent–solvent correlations. The three experiments are made with (a) $(CD_3)_3COD$ in D_2O, (b) $(CD_3)_3COH$ in H_2O and (c) 50:50 $(CD_3)_3COH/(CD_3)_3COD$ in 50:50 H_2O/D_2O.
2. Solute–solute distribution functions are probed through substitution on the alcohol methyl hydrogen sites to yield the (partial) radial distribution functions $g_{HH}(r)$, $g_{HX}(r)$ and $g_{XX}(r)$ for the solute–solute correlations. The three experiments are made with (a) $(CD_3)_3COD$ in D_2O, (b) $(CH_3)_3COD$ in D_2O and (c) 50:50 $(CD_3)_3COD/(CH_3)_3COD$ in D_2O.
3. Solute–solvent distribution functions are probed through substitution on the alcohol methyl hydrogen sites and the water hydrogen sites. In combination with the solute–solute and solvent–solvent distribution functions, this yields the (partial) radial distribution functions $g_{HH}(r)$, $g_{HX}(r)$ and $g_{XX}(r)$ the solute–solvent correlations. The three experiments are made with (a) $(CH_3)_3COH$ in H_2O, (b) $(CD_3)_3COD$ in D_2O and (c) 50:50 $(CD_3)_3COD/(CH_3)_3COH$ in 50:50 H_2O/D_2O.

Thus we appear to have specified nine isotopically distinct experiments. However, we note that samples 1(a), 2(a) and 3(b) are identical. We therefore perform only 7 experiments to yield the 9 (partial) radial distribution functions specified above, namely $g_{HH}(r)$, $g_{HX}(r)$ and $g_{XX}(r)$ for each of the solvent–solvent, solute–solute and solute–solvent cases considered.

2.4. Extracting all the partial rdfs

Despite the fact that we have only performed seven different experiments, we can use these data,

together with other known chemical information, to extract the partial radial distribution functions we require. This is not a case of getting something for nothing—it is doing the same sort of thing as a crystallographer does when refining a crystal structure in which the number of independent reflections is—as is usually the case for large molecules—less than the number of structural parameters that need to be refined. The crystallographic refinement is constrained by what we know of the chemistry of the system (e.g. standard bond lengths and angles, non-overlap of atoms). In effect, we do something similar in the liquid case.

The procedure used—the Empirical Potential Structure Refinement (EPSR) technique developed by Soper [7]—produces model ensembles of molecules that are consistent with the observed scattering. These ensembles can then be interrogated to see the detailed geometries of the various intermolecular interactions in a given solution—essentially obtaining the full molecular structure of the solution. The procedure starts by running a Monte Carlo simulation of the system using a set of standard potential functions $U^0_{\alpha\beta}(r)$. After an initial equilibration time, the various partial radial distribution functions $g_{\alpha\beta}(r)$ for the simulated system are estimated. This in general (in all cases we are aware of so far) fails to give adequate agreement with experiment, indicating in passing that the starting potentials—which are used extensively in simulations of a range of chemical and biological systems—are inadequate to reproduce the experimental data. So the initial potential energy function is then modified by adding sets of potentials of mean force between the various different sites. These are derived from comparing the experimental and the simulated $g^D_{\alpha\beta}(r)$ rdfs. Thus, we obtain a modified potential set:

$$U^N_{\alpha\beta}(r) = U^0_{\alpha\beta}(r) + kT\ln\left[\frac{g_{\alpha\beta}(r)}{g^D_{\alpha\beta}(r)}\right]. \quad (4)$$

This new potential function set is fed into the system and a further simulation calculation performed. The above procedure is then repeated until $U^0_{\alpha\beta}(r) \sim U^N_{\alpha\beta}(r)$ and $g_{\alpha\beta}(r) \sim g^D_{\alpha\beta}(r)$ for all r and for all pairs of atoms α,β. All of the tests that have been done to date using this procedure [8] indicate strongly that forcing the simulated molecular ensembles to reproduce the measured radial distribution functions is a substantial constraint on the three-body and higher-order correlation functions, and hence captures the essential topology of the local order. The resulting experimentally consistent ensembles can then be interrogated to obtain site–site partial radial distributions to examine the detailed structure of the system. Note that what is described above is an earlier implementation of EPSR which operated in real space—i.e. the comparisons were made between partial radial distribution functions. The normal implementation is now in reciprocal space—i.e. using the partial structure factors $S_{\alpha\beta}(Q)$ to modify the potential.

In passing, we can note that the way in which the potential function is modified to bring the simulation into agreement with the experiment may be able to guide us in improving the potential functions originally used in the system—or at least give us an idea of what aspects of the starting potentials need modification. An example is a study of pure liquid *t*-butanol [9], where the starting potentials showed a degree of hydrogen bonding between the molecules to be about double that which was consistent with the experimental structural results. The implication of this was that the standard potential functions used as a starting point for the EPSR refinement procedure overemphasised the alcohol–alcohol hydrogen bonding term at the expense of the alcohol–water interaction. However, we would underline that EPSR is not a technique that can easily be used to quantitatively refine potential functions.

3. Structure at the microscopic level

Once we have these ensembles of molecules that are consistent with the experimental data, we can extract detailed structural information. This obviously includes complete partial rdf information as indicated above. However, because we have coordinate data, we can also obtain information on how various molecules are both arranged spatially around any other molecule or atom type (essentially breaking the spherical averaging in the rdf), and also how these neighbouring molecules are

oriented around a given molecule or atom. We will use some of these functions in what follows but without full definitions. The full hierarchy of functions that can be used is described in Ref. [10].

3.1. The structure of the hydration shell

Perhaps the earliest diffraction experiment that was successful in extracting structural information on the hydration shell of a non-polar group was that on a 1:9 solution of methanol in water [11]. This work established the ability of the technique to detect subtle structural differences in liquid structures, an ability that has since been considerably enhanced with subsequent advances in data collection and analysis techniques (for example, see [9,10,12–18]). Two main pieces of relevant evidence were obtained. First, the dominant orientation of the water molecules surrounding the non-polar groups was with their dipole moments preferentially aligned tangential to a sphere imagined to be centred on the methyl group carbon. Referring to Fig. 1, this is exactly what would be expected in a clathrate-type arrangement. However, the orientational correlation function data obtained showed that there was considerable disorder in the structure, and that it would be misleading to regard this cage as being strongly ordered—we are after all dealing with a liquid, and as such we would expect a significant degree of disorder. Thus, these results first verified—through the dominant water molecule orientations—that the hydration structure was indeed related to that of the 'classical' clathrate cage model. But secondly—and importantly—they stressed that there was considerable disorder in the structure.

Further evidence for the deviation of this structure from the ideal clathrate cage came from EXAFS measurements on a fully non-polar atom, Krypton, in water. By tuning the experimental conditions, it was possible to measure the EXAFS (a) in the solution just above the freezing line, and (b) in the crystal just below the freezing line [19]. The solution and crystal Kr–O rdfs in Fig. 2 show the higher degree of ordering in the hydration shell of the solid through the sharper features of the crystalline radial distribution function. These

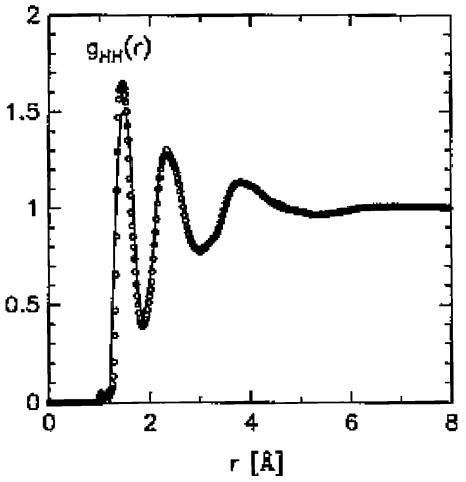

Fig. 3. The hydrogen–hydrogen partial rdf for a 1:9 mole fraction solution of methanol in water (line) compared to the same function for pure water (circles).

results are fully consistent with the conclusions drawn from the neutron data [11] that the average orientational configurations of the water molecules in contact with the gas in the liquid state deviate significantly from the largely tangential orientational configurations of the clathrate cage structure. A hydration 'cage' may exist in the liquid, but it is more loosely defined than in the solid-state system that is the classical model for the non-polar hydration shell. The isotope substitution measurements on Argon in water of Broadbent and Neilson [20] are also consistent with these conclusions, as can be seen from the width of their Argon-water radial distribution function. At the time of their measurements, the techniques available for interpreting the data were much more limited, so they were unable to extract the detailed information that is now possible.

How then can we quantify the degree to which the water structure in the hydration shell deviates from the bulk structure? This is the second piece of relevant information that we can obtain from the neutron experiment discussed above [11]. The hydrogen–hydrogen rdf can be extracted from the data, and compared to the same function for bulk water. The comparison is shown in Fig. 3, and the message is striking: the two functions are essen-

tially indistinguishable. We are therefore forced to the—initially surprising—conclusion that, as far as this measurement of structure is concerned (which is a sensitive one that includes all-important orientational information), the structure in the hydration shell looks remarkably similar to that in the bulk. There is no obvious perturbation of the structure in the direction of increased—or indeed of decreased—ordering. Similar conclusions have been drawn more recently in a range of independent studies of other molecules containing nonpolar head groups [12,13,21]. It seems that we must forget the 50-year-old standard model and look elsewhere for a structural source of the entropic driving force for the hydrophobic interaction.

3.2. The water's environment: second shell ordering

The *spatial density function* describes how the molecules surrounding a central molecule are distributed. Imagine sitting on a molecular site in liquid water—say on the oxygen of a water molecule—and looking around at the neighbouring water molecules at different distances. We will notice that there is a preference for neighbouring water oxygens, not only at certain radial distances corresponding to the maxima in the OO partial rdf $g_{OO}(r)$, but also that these preferred neighbours are to be found in those particular directions that reflect the orientational dependence of the intermolecular interactions (the hydrogen bond in pure water). We can then construct a further pair distribution function to describe this orientational preference of a particular direction as a function of the distance from the central atom. This is the *spatial density function* (sdf) [22], which gives us orientational information on the positioning of the neighbouring atoms. What we are in effect doing is assigning locations on a surrounding sphere—essentially a latitude and a longitude—for the distribution of neighbouring molecules. Formally, the sdf $g_{\alpha\beta}(r,\Omega)$ represents a three-dimensional map of the density of β sites as a function of radial distance, r, and orientation Ω about a central site α.

When we look at the sdf of water in the bulk liquid and in a 0.06 mole fraction aqueous *t*-butanol solution (the thermodynamics of which is thought to confirm its behaviour as being dominated by hydrophobic interactions [23]), we observe an unexpected difference. The sdfs of bulk water, and of the aqueous *t*-butanol solution at room temperature and 65 °C are shown in Fig. 4. We emphasise that we are looking here at the *water* neighbourhood of the *water*, not of the nonpolar group.

Focussing first on the first neighbour shells in the top panels, we see the standard spatial density function for the first neighbour shell in water. The two lobes above the central water relate to neighbouring waters that accept hydrogens from the central molecule, while the broad lobe beneath indicates waters donating hydrogens to the lone pair region of the central water. This first neighbour shell is unchanged in both the room temperature and elevated temperature *t*-butanol solutions.

When we look at the second shells in the bottom panels, we see some clear differences between the bulk and the solutions, and between the two different temperatures of the solution. Although the basic geometry of the second shell is similar in all four cases, we see that the second shell is progressively 'pulled in' toward the central molecule as we move from bulk water to the 25 °C solution. There is a progressive narrowing of the band in the centre of the bottom panels of Fig. 4 as we move from left (bulk water) to right (65 °C 0.06 *t*-butanol). Consequently, lobes of spatial density corresponding to the third shell begin to appear in the two solution plots. Furthermore, the lobe directly below the central molecule changes from circular to ellipsoidal in going from bulk water (left) to solution (middle).

This 'drawing-in' of the second shell is accompanied by a significant ordering of the waters in the shell—in effect these waters occupy a smaller volume in the solution. This we can see more clearly by rotationally averaging the sdfs of Fig. 4. Fig. 5 gives these rotational averages for the three cases, where we can indeed see the second shell structural tightening induced by the presence of the alcohol molecule in the breaks of continuity in the 10 o'clock and 2 o'clock directions as we

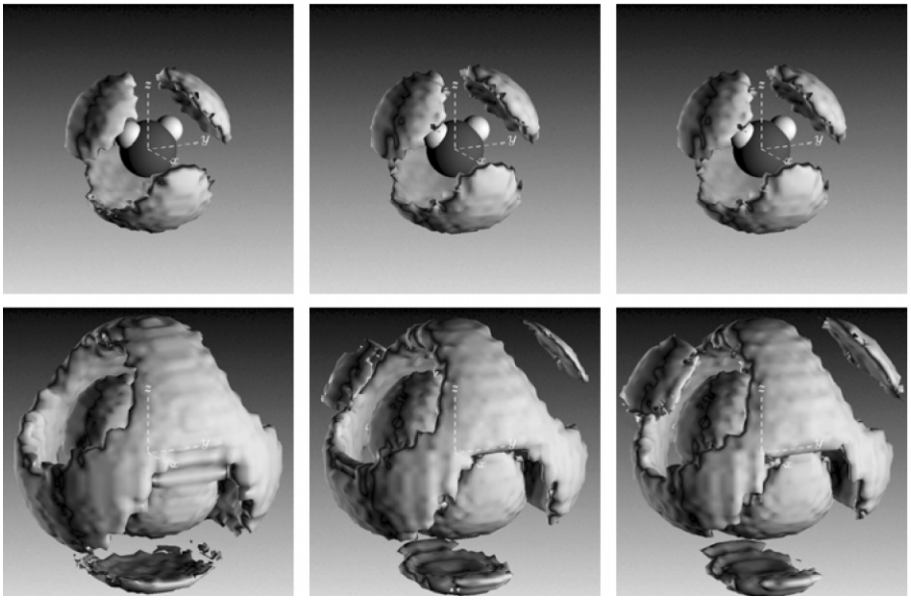

Fig. 4. The spatial density functions of water molecules around a central water molecule for (top row) first neighbour shell water molecules and (bottom row) first and second shell waters. In turn the panels show the distributions for (left) pure water at 25 °C, (centre) 0.06 mole fraction *t*-butanol-water solution at 25 °C and (right) 0.06 mole fraction *t*-butanol-water solution at 65 °C. The first shell of neighbours (top row) illustrates the invariance between the three systems of the short-range first neighbour correlations that are of a predominantly tetrahedral local water co-ordination. The appearance of the third neighbour shell in the direction of the central molecule O–H bonds for the alcohol-water mixtures (bottom centre and bottom right) visibly illustrates the solute-induced compression of the solvent molecular density, which appears to be enhanced by increasing temperature.

move from bulk water to the two solutions. Also visible is the small but significant inward shift of the lobes, which is particularly obvious in the 12 o'clock direction. Taking sections through the appropriate lobes allow us to quantify both these inward shifts and the narrowing of the shell widths [13]. In terms of the water molecule's second neighbour shell, we have clear evidence that the presence of *t*-butanol increases structural order in the system. This ordering is enhanced with the rise in temperature to 65 °C, paralleling the known increase in the hydrophobic interaction as we raise the temperature. Furthermore, the change in the shape of the bottom lobe from circular to ellipsoidal also suggests further localisation of the second shell waters in the solution.

Perhaps it is here—in the *water's second* shell rather than the *alcohol's first* hydration shell—that the entropic driving force for the hydrophobic interaction is to be found. There certainly is some ordering of the water, but not in the hydration shells of the non-polar groups where the standard model would tell us to look [13,17].

3.3. Molecular segregation

Small alcohols—up to *t*-butanol—are miscible with water in all proportions. Perhaps because of this, it is generally accepted that water and alcohol molecules in these solutions are randomly mixed. That the entropy of the system, on mixing, increases less than expected for an ideal solution of randomly mixed molecules is well known [24]. As discussed earlier, this effect is usually attributed to the non-polar headgroups 'ordering' the surrounding water, i.e. to hydrophobic hydration [2].

For the aqueous solutions we are discussing here, we have essentially complete structural data. So far we have considered only the water structure around the non-polar headgroups (solute–solvent

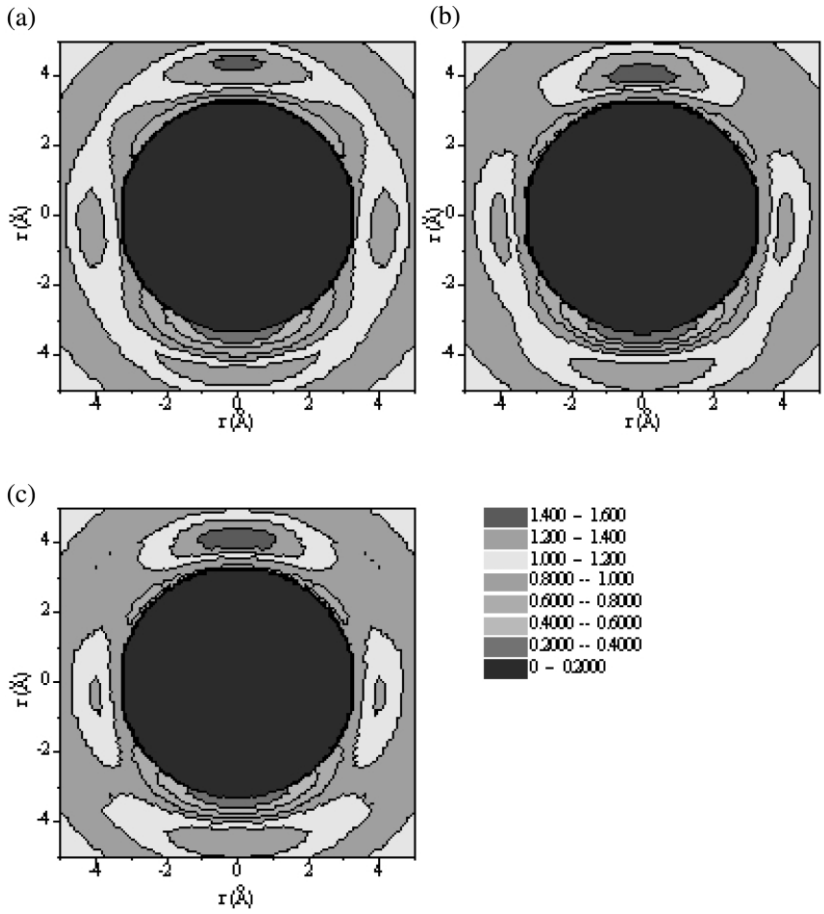

Fig. 5. Two-dimensional maps of the second water shell spatial density functions of Fig. 4. These are obtained by rotationally averaging $g_{OO}(r,\Omega)$ about the z-axis. The map in (a) corresponds to pure water at 25 °C, in (b) to 0.06 mole fraction *t*-butanol-water solution at 25 °C and in (c) to the alcohol solution at 65 °C. The disruption—i.e. increased localisation—of the second shell water in the presence of the alcohol molecule can be seen in the two o'clock direction: this perturbation is also marked by the inward migration of the shell, in particular along the twelve o'clock direction.

interactions, or hydration) and the solvent–solvent structure. But we can also examine the interactions between the solute molecules. Thus we can investigate the chemical nature of the solute–solute interactions, and observe how these are affected by changes in solvent composition, temperature and even pressure. Much of this detail, which shows that the solute alcohols interact almost entirely via direct contacts between their non-polar head groups, as would be expected for systems controlled by the hydrophobic interaction, has been written up elsewhere [12,13,17].

We limit ourselves here to considering size effects consequent on the solute–solute interaction. Fig. 6 shows one of the 28 partial rdfs relating to solute–solute correlations obtained for the *t*-butanol-water system at three concentrations. For all three concentrations there is a broad peak centred between 5.5 and 6.0 Å. This peak position tells us immediately that there is *direct* contact between neighbouring *t*-butanol molecules. As shown by recent work at 0.02 mole fraction [15], this is true even at this lowest concentration. The molecules

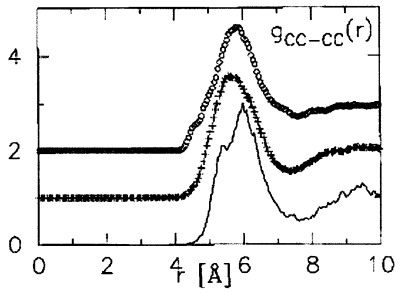

Fig. 6. The molecular centres function $g_{CC-CC}(r)$ for 0.16 (○), 0.11 (+) and 0.06 (−) mole fraction *t*-butanol in water.

are not separated by an intervening solvent layer [25].

Moreover, the area under this peak tells us how many molecules on average surround a central solute molecule: it rises from 2.8 ± 0.6 at 0.06 mole fraction, through 4.4 ± 0.6 at the intermediate concentration, to 5.8 ± 0.6 at the highest 0.16 mole fraction concentration. Again referring to the very recent results for the 0.02 mole fraction system [15], a coordination number of 1.5 ± 0.7 indicates that even at this concentration—below the minimum in the partial molar volume—a significant degree of solute association is found. There is thus clear structural evidence here of some molecular segregation, of some tendency to what we might call 'microscopic phase separation'.

This tendency to molecular segregation has been quantified in detail in a study of a concentrated methanol–water solution [16]. If water and methanol were randomly mixed at the molecular level, most water would exist as isolated molecules at this concentration, with distinct water clusters being rare. In practice although single water molecules do occur, these constitute only approximately 13% of all the water molecules in the mixture. The remaining 87% occur in clusters or strings containing 2 to 20 or more molecules, with the most likely structure being a 3-water molecule cluster. A snapshot of the simulation box (Fig. 7) shows groups of water molecules hydrogen bonded together, forming small cavities in a 'fluid' of methyl headgroups. In this image, two water clusters can be seen left of centre and centre right, hydrogen-bonded to the hydroxyl groups of surrounding methanol molecules. The function of hydroxyl groups as bridges between methyl headgroups and water clusters explains another experimental finding [16]: why on average the methanol hydroxyl groups are further apart in the solution than in pure methanol.

Again, these results are not limited to a single system—similar microsegregation behaviour has also been observed (Fig. 8) in a concentrated (6:1) *t*-butanol-water solution [14]. This suggests the phenomenon is not limited to the methanol system, but is likely to be general for small alcohols.

This is a further piece of direct structural evidence that challenges the standard interpretation of the entropy of mixing [2] in solutions of molecules containing non-polar groups: contrary to speculation that water structure is either enhanced or destroyed in an alcohol solution [23,26], these results show that the local structure of water even in a concentrated methanol-water solution is surprisingly close to its counterpart in pure water. Whilst the entropy of mixing cannot be calculated directly from these structural results, they do imply that the negative excess entropy observed in these systems [2,26] arises from incomplete mixing at the molecular level, rather than from water restructuring. There are similar suggestions based on non-structural measurements [27] and simulations [28].

Furthermore, as we have complete experimentally-consistent structural information on these solutions, the degree of hydrogen bonding in the mixture can be calculated and compared to that in the two liquids before mixing. For the mixture, the average number of hydrogen bonds per molecule is unchanged from the number that would be found in the same relative amounts of pure liquids prior to mixing [16]. The hydrogen bonds between methanol and water molecules created upon mixing thus compensate almost exactly for the water—water and methanol—methanol hydrogen bonds lost upon mixing the pure liquids. It can therefore be further suggested that the sign and magnitude of the excess enthalpy of mixing will be determined by an interplay between the relative strengths of the alcohol–alcohol, alcohol–water and water–water hydrogen bonds, since the number of hydrogen bonds per molecule in solution is

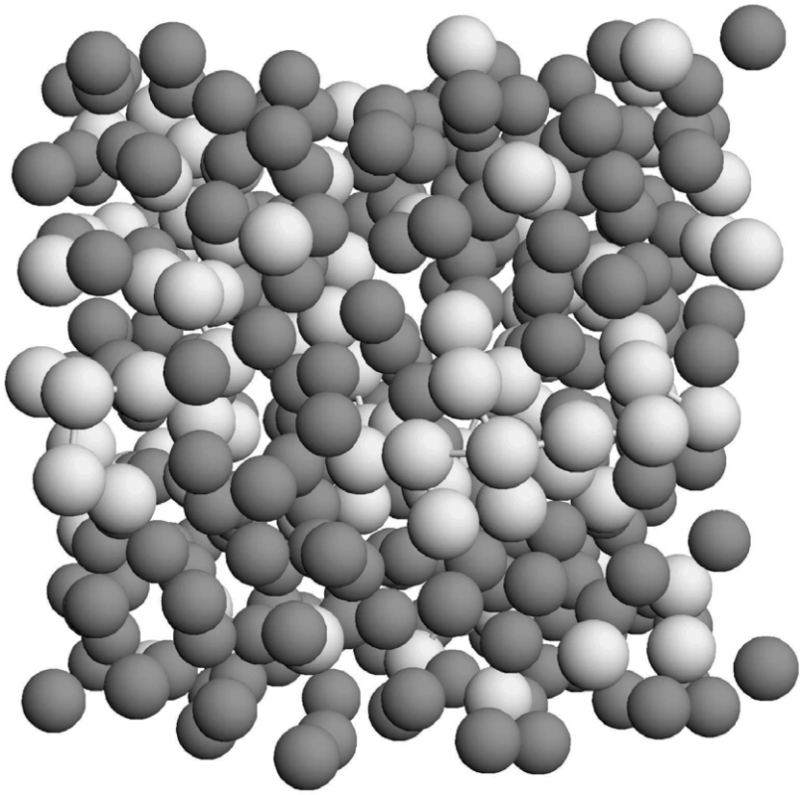

Fig. 7. One of the simulated molecular boxes of a 7:3 molar ratio solution of methanol in water. Methyl groups are shown as grey spheres. Larger light spheres have been used to highlight the positions of water molecules. Bonds join water oxygen atoms to other oxygen atoms within their first coordination shell ($r < 3.5$ Å).

not significantly different from that in the pure liquids prior to mixing. The polar interaction of water with the alcohol hydroxyl group is thus likely to be a far more potent influence on the thermodynamic properties of alcohol-water mixtures than any water restructuring induced by the hydrophobic methyl groups.

4. Structure at the mesoscopic level

We conclude with some new results relating to the mesoscopic level behaviour of aqueous amphiphilic systems that relate to the hydrophobic interaction. These follow on directly from the incomplete mixing discussion in the preceding section. Using small angle neutron scattering (SANS), a technique that measures fluctuations in neutron scattering density over distance scales significantly greater than the molecular level we have been discussing so far, we can obtain information that not only complements the above results, but also tells us how the molecular clusters induced by the hydrophobic—or other—interactions change with temperature and concentration. Although we shall see that at certain concentrations the temperature dependence parallels the expected behaviour of the ‘strength’ of the hydrophobic interaction, the concentration differences suggest a more complex situation in which a subtle balance of polar and non-polar interactions may be involved.

Experimental evidence for the existence of longer range structural correlations in dilute tertiary butanol-water solutions was obtained initially with

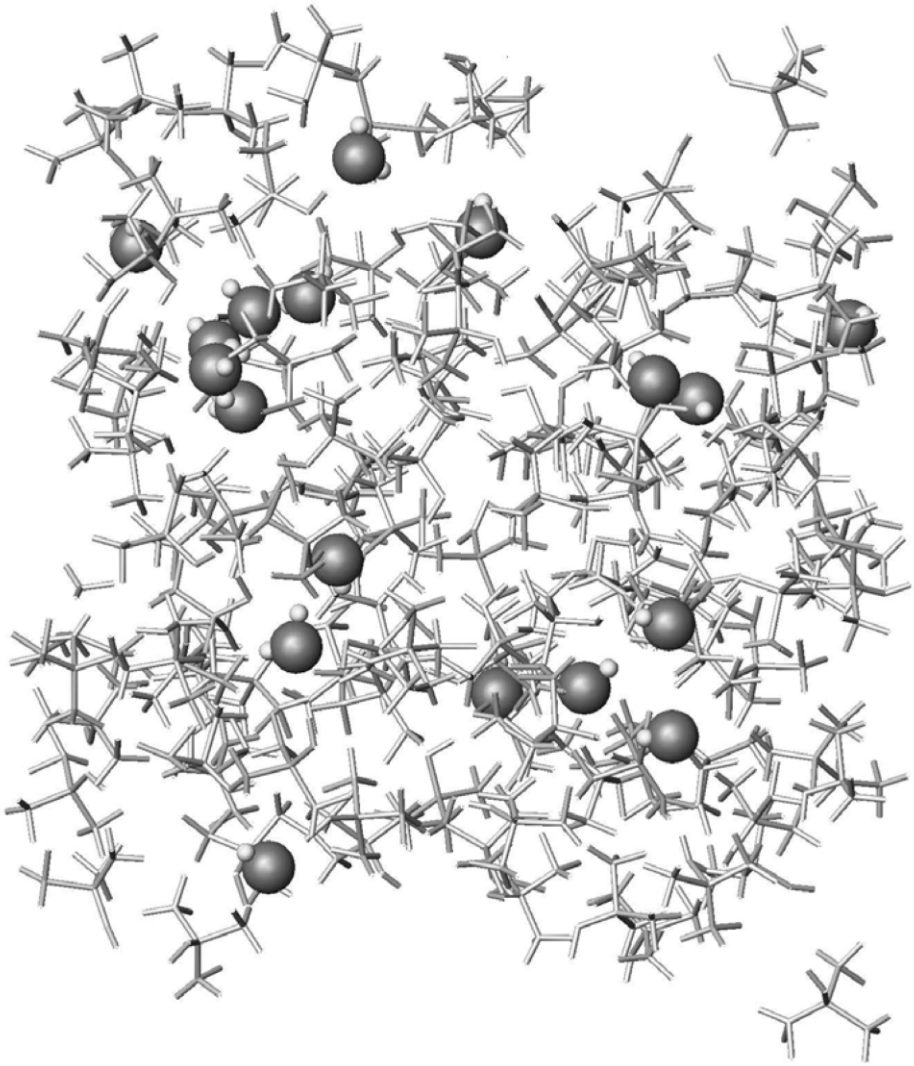

Fig. 8. Snapshot of the structure of a 0.86 mole fraction *t*-butanol-water solution. For clarity and to enhance the visibility of pockets of water molecules, the *t*-butanol molecules have been rendered as stick models, and the water molecules as ball and stick models.

techniques such as light scattering [29,30] and small angle X-ray scattering [31]. These early results, though suggesting that some form of in-solution mesoscale structural fluctuations did occur, had little specific structural sensitivity to the detailed distribution of the fluctuations between the two mixture components. This was due to the fact that both of these techniques effectively measure fluctuations in the electronic density of the liquid mixture for which there is little contrast between the solvent water and the solute alcohol molecules. The neutron scattering methods applied here have considerable advantages over X-rays for the study of the mesoscopic structure in these liquids. This is because once again we can take advantage of the large difference in the scattering power of hydrogen as compared to deuterium. Combining this with our ability to selectively label either the alcohol or the water molecules we can

enhance the technique's sensitivity to either the alcohol or the water component.

The rationale for these measurements relates directly to Kauzmann's 1959 paper [1] arguing that hydrophobic interactions are the major driving force stabilising the three dimensional structure of proteins. They are therefore thought central to their viable functioning. With the discovery of organisms growing at up to 113 °C, much interest in protein stability has focussed on proteins from these organisms, many of which are stable above 100 °C in vitro. Part of this interest is biotechnological, and includes efforts to engineer increased stability into industrially useful proteins. This work is technically demanding and potentially tedious, and a significant deterrent is the expectation that proteins cannot be stable above 140 °C, based on what is known of the effect of temperature on the hydrophobic interaction. The interaction is known to increase in strength up to approximately 70 °C, and decline above this temperature. Although there is no direct evidence of the effect of temperature on the hydrophobic interaction above 80 °C, based on extrapolation and theory it is expected that this decline above 70 °C is such that above 140 °C the hydrophobic interaction will make no contribution to protein stability, and therefore that proteins stable near this temperature are unlikely, and above it are impossible [32,33]. Thus, the main reasons for believing there is an upper limit to protein conformational stability are not based directly on experimental data. However, earlier extrapolations gave an upper temperature limit for protein stability of approximately 115 °C [34]. We now know of proteins with significant lifetimes at 125 °C, and it has been argued that this limit has been set by the growth temperature of the source organism rather than by any inherent limit on stability [35].

The aim of this work was thus to obtain experimental information on the strength of the hydrophobic interaction at elevated temperatures relevant to thermophilic organisms, and in particular to obtain experimental evidence for the postulated rate of decline of the hydrophobic interaction above 70 °C. From this we would expect to be able to make better estimations of the likely upper temperature limit for protein stability.

4.1. Experimental

In an attempt to measure the mesoscopic structural consequences of the hydrophobic interaction, the changes in density fluctuations in the *t*-butanol-water system with temperature were followed using small angle neutron scattering. To study the mesoscopic structural fluctuations from the viewpoint of the alcohol molecules, small angle neutron scattering data were collected from mixtures of protiated tertiary butanol, $(CH_3)_3COH$ in D_2O, at three concentrations of 0.02, 0.04 and 0.06 mole fraction alcohol. This covers the concentration range in which the sharp minimum in the partial molar volume of tertiary butanol in tertiary butanol-water mixtures occurs [36], and that is also consequently associated with the believed maximum in the hydrophobic effects manifest in the liquid mixture [23]. To investigate the temperature dependence of any long-range structural correlations, data were also collected between 20 and 160 °C so as to cover the range over which hydrophobic effects are thought to pass through a maximum [37].

Data were collected at the D22 Small Angle Neutron Diffractometer at the Institute Laue-Langevin, Grenoble, France. At the time of the experiment the instrument was configured to collect data over the Q-range from 0.00275 to 0.04335 $Å^{-1}$, using neutrons of wavelength 10 Å. Very approximately this Q-range corresponds to probing length scales ranging from approximately 2300 Å down to 150 Å (using the relation that the length scale $\sim 2\pi/Q$). The alcohol–water samples were prepared by making appropriate mixtures of outgassed alcohol and (deuterated) water. They were transferred to 2 mm path length quartz cells, specially designed to take the increase in pressure as the solutions were heated above the boiling point of the liquid mixture. These cells, specially manufactured by Hellma, were mounted in an automatic sample changer and the temperature was controlled by means of a thermostatic water bath heating the frame to which the cells were attached. All data were corrected for empty cell scattering and normalized to the incoherent scattering level of H_2O.

4.2. Results

In all the systems investigated, the small angle scattering from each sample is seen to increase only below a value of $Q = 0.015$ Å^{-1} suggesting that correlation lengths of upwards of several hundred of Ångstroms exist in the systems. The temperature dependence of this scattering at the three concentrations shown in Fig. 9 immediately suggests that some intriguing intermolecular interactions must be occurring. At the lowest measured concentration, 0.02 mole fraction alcohol, the small angle scattering of the sample remains small and constant as the temperature is raised from 40 to 140 °C. In contrast, in the most concentrated solution measured, 0.06 mole fraction, considerable small angle scattering is visible from room temperature up to 120 °C, but it then falls away to almost nothing above this temperature. For the intermediate concentration, 0.04 mole fraction, a comparison with these other two concentrations highlights some quite remarkable temperature dependent scattering. The signal is seen to increase from a value smaller than that of the 0.02 mole fraction system at room temperature to a maximum that is approximately four times greater than the most dilute case at 100 °C. This peak in the scattering level is also slightly greater than found in the more concentrated solution at the same temperature. The scattering then falls away with increasing temperature in a manner similar to that found in the 0.06 mole fraction solution.

4.3. Discussion

How can these observations be understood? A simple interpretation would suggest that at the most dilute concentration measured, the degree of mesoscopic length scale structure between alcohol molecules remains small but constant over the investigated temperature range. At 0.06 mole fraction alcohol there is considerably more inter-alcohol mesoscopic structure present in the solution (as seen in the high angle scattering results discussed in the previous section), but again as a constant component within the solution below a temperature of 120 °C. Above this temperature the solution appears to become homogenised on the length scales investigated. The intermediate concentration of 0.04 mole fraction alcohol appears the most interesting. As the temperature is increased from ambient the degree of mesoscopic length scale solution structure is seen to increase from a level below that of the 0.02 mole fraction solution where the liquid mixture appears almost completely homogenous across the probed length scales. This then increases to pass through a considerable peak in alcohol–alcohol correlations that occurs at approximately 100 °C and which falls away above this temperature to an almost perfectly homogenous solution state above 120 °C. These results suggest that concentration dependence of the balance of the intermolecular forces that govern these solutions is crucial to the magnitude and temperature dependence of the long-range structural correlations, and each solution will have to be characterised independently. The question as to what is the precise structural origin of the long-range correlations remains difficult to answer. Though the isotopic contrast enhancement allows us to assume that in some way these long-range correlations relate directly to the distribution of alcohol molecules within the system, it does not tell us whether the scattering is from individual large structural entities that have the characteristic large correlation length, or whether it is from long-range correlations between smaller structural entities i.e. is the solution de-mixed on the longer length scales or are microclusters of alcohol molecules correlating over large distances? The fact that the scattering functions are flat between 0.015 and 0.04 Å^{-1} seems to suggest that if the latter hypothesis is valid, the size of the small alcohol clusters must be less than 145 Å as there is no obvious small angle scattering signal in the range from there up to $\gg 400$ Å.

The room temperature baseline intermolecular structure has already been characterised for the 0.02 [15] and 0.06 mole fraction [12,13] solutions. A comparison between these detailed results has shown that in the more dilute solution the alcohol molecules tend to remain either as free molecules or as linear alcohol dimers interacting through head-to-head non-polar group to non-polar group contacts [15]. At the higher concentration of 0.06 mole fraction, the degree of orientational ordering

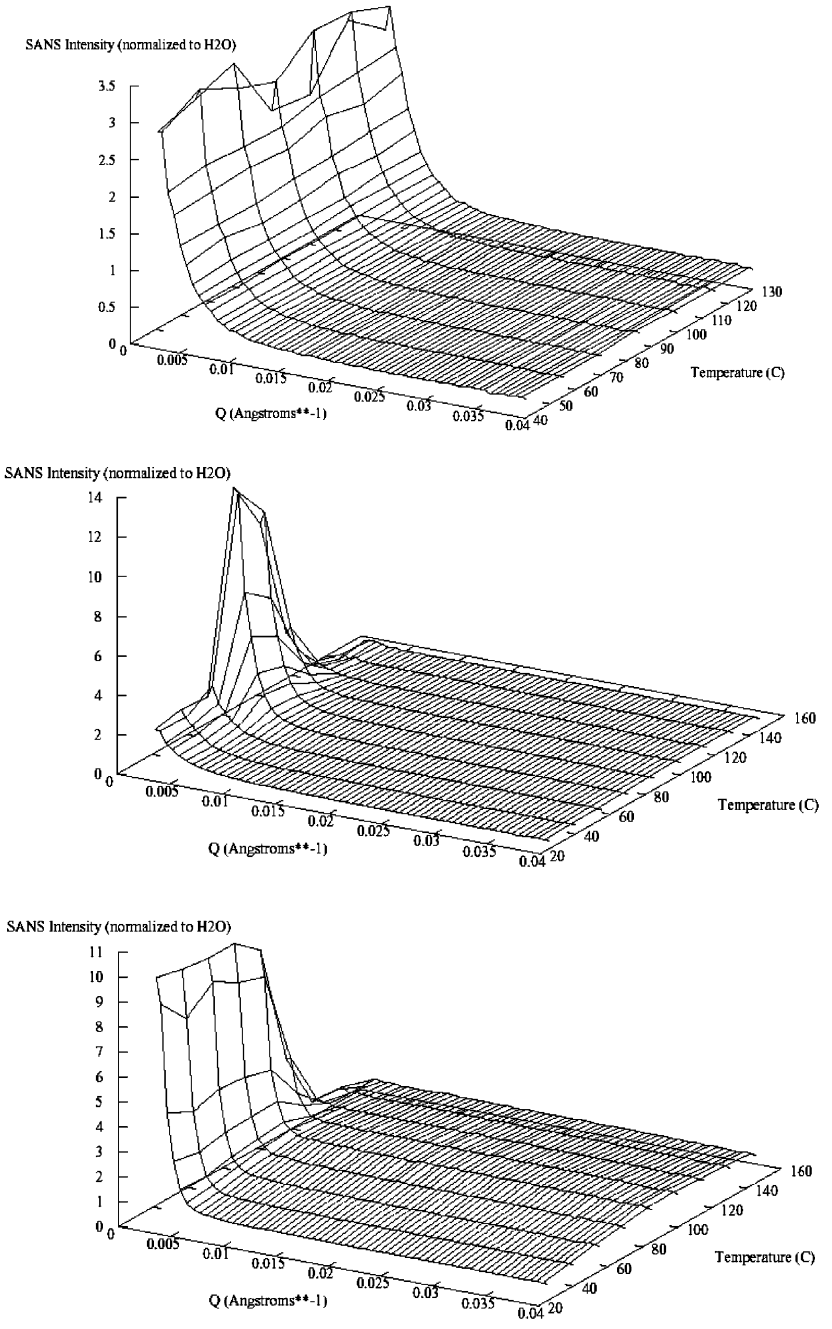

Fig. 9. The small angle scattering of solutions of *t*-butanol in water as functions of temperature; (top) 0.02 mole fraction; (middle) 0.04 mole fraction; (bottom) 0.06 mole fraction.

between associated alcohol molecules is more diverse with the average cluster size for alcohol association being three to four molecules [13]. The molecules in these molecular clusters still tend to interact through non-polar group to non-polar group interactions. The room temperature short range inter-alcohol correlations at 0.04 mole fraction alcohol are yet to be determined, though in the light of the mesoscopic length scale structural correlations that are observed here, this information will be vital in trying to understand this complex mesoscopic behaviour. How these short to medium range intermolecular correlations then assemble into the mesoscopic structural entities that give rise to the marked small angle scattering remains to be explained. Techniques to directly address this challenging question are currently being developed.

On the basis of these initial results, it may be tempting to suggest that the strong maximum in the small angle neutron scattering observed at ~80 °C, and its fall-off to ~0 at apprioximately 120–140 °C, reflects the expected temperature dependence of the hydrophobic interaction. If we accept this, then if protein conformational stability is strongly dependent on the hydrophobic interaction, then thermophilic proteins will not be found at temperatures much above 120 °C. However, the complex temperature and concentration dependences of the clustering observed suggest that a complex balance of hydrophobic and hydrophilic interactions—already seen in the high angle scattering data—needs to be unravelled. Until that is done by further work, it would seem premature to try to draw firm conclusions about the relationship of these results to protein conformational stability at high temperatures. The richness of behaviour observed does however suggest that such work could reveal interesting and relevant new conclusions about interactions of amphiphiles in aqueous solution in general which are likely to be of significant relevance to biomolecular stability and interactions in particular.

5. Conclusions

Neutron scattering isotope substitution methods have allowed us to open up a new window on the molecular structures of aqueous solutions. As applied to aqueous amphiphiles whose behaviour is believed to be driven by hydrophobic interactions, we can now see the structures of the hydration shells of non-polar groups, and hence test the classical ‘water ordering’ explanation of the entropic driving force of the hydrophobic interaction. Moreover, the chemical nature of the solute–solute interactions in these systems—the apparent consequences of the hydrophobic interaction—can also be seen directly as functions of temperature and concentration.

Although the hydration shell of non-polar groups bears a superficial resemblance to the clathrate cage structure to which ‘ordered water’ is often likened, the disorder in this organisation is significant. The direct comparison with the actual crystalline cage made using EXAFS shows graphically the considerable differences between this ‘reference’ cage structure and the real liquid hydration shell. Moreover, when the hydration shell structure is looked at from the water’s viewpoint, there is no evidence to suggest that the water structure here is significantly different from the structure of bulk water. Thus, expulsion of hydration water to the bulk liquid would appear not to provide a structural source of the entropic driving force of the hydrophobic interaction.

Interesting water ordering effects are however found, but in a different region from that expected, namely in the second neighbour shell of the water molecule. Moreover, although small alcohols are fully miscible with water, a property that has led us to assume that these solutions are well mixed, experimental measurements show clearly that there is significant clustering. Whether either or both of these two effects—water second shell ordering and microclustering—can provide the entropic driving force for the hydrophobic interaction remains to be seen. Furthermore, we can see clearly the chemical nature of the solute–solute contacts, which are seen to be almost wholly made through direct non-polar to non-polar contacts, with almost no intermolecular hydrogen bonding. In addition, the measurements allow us to quantify changes in numbers of hydrogen bonds as alcohol concentration is varied, thus offering insight also into the possible structural sources of the mixing enthalpy.

Small angle neutron scattering measurements enable us to quantify density changes—which reflect clustering at longer, mesoscopic length scales—as functions of temperature and concentration. Initial results at the low concentration end of the *t*-butanol-water system show a rich and complex behaviour that cannot be interpreted simply in terms of the expected temperature dependence of the hydrophobic interaction. While at 0.04 mole fraction—close to the minimum in the partial molar volume at which hydrophobic effects are thought to be maximised—the small angle scattering passes through a maximum at ~80 °C, the different behaviours at both lower and higher concentrations suggest we should be wary of drawing simple conclusions concerning the role of the hydrophobic interaction, for example with respect to the stability limits of thermophilic proteins. As for proteins, the structures of amphiphile solutions seem to be controlled by a complex balance of polar and non-polar interactions, and further work is needed to try to understand this balance—and its role in biomolecular stability and interactions—more deeply.

Acknowledgments

We thank the ISIS Facility and the Institut Laue-Langevin (ILL) for neutron beam time, and the European Synchrotron Radiation Facility for access to synchrotron radiation. We thank Peter Lindner and David Bowyer of the ILL for provision and testing of the pressure resistant cells used in the small angle scattering measurements.

References

[1] W. Kauzmann, Some factors in the interpretation of protein denaturation, Adv. Protein Chem. 14 (1959) 1–63.
[2] H.S. Frank, M.W. Evans, Free volume and entropy in condensed systems, iii. entropy in binary liquid mixtures; partial molal entropy in dilute solutions; structure and thermodynamics in aqueous electrolytes, J. Chem. Phys. 13 (1945) 507–532.
[3] D.W. Davidson, in: F. Franks (Ed.), Water—A Comprehensive Treatise, 2, Plenum Press, New York, 1973, p. 115.
[4] E. Sloan, Clathrate Hydrates of Natural Gases, Marcel Dekker, New York, 1990.
[5] C. Folzer, R.W. Hendricks, A.H. Narten, Diffraction pattern and structure of liquid trimethylamine decahydrate at 5 °C, J. Chem. Phys. 54 (1971) 799–805.
[6] F.G. Edwards, J.E. Enderby, R.A. Howe, D.I. Page, The structure of molten sodium chloride, J. Phys. C 78 (1975) 3483–3495.
[7] A.K. Soper, Empirical potential monte carlo simulation of fluid structure, Chem. Phys. 202 (1996) 295–306.
[8] A.K. Soper, Tests of the empirical potential structure refinement method and a new method of application to neutron diffraction data on water, Mol. Phys. 99 (2001) 1503–1516.
[9] D.T. Bowron, A.K. Soper, J.L. Finney, The structure of pure tertiary butanol, Mol. Phys. 93 (1998) 531–543.
[10] J.L. Finney, D.T. Bowron, in: S.F. Billinge, M.F. Thorpe (Eds.), From Semiconductors to Proteins: Beyond the Average Structure, Kluwer Academic/Plenum, 2002, p. 219.
[11] A.K. Soper, J.L. Finney, Hydration of methanol in aqueous solution. Phys. Rev. Lett. 71 (1993) 4346–4349.
[12] D.T. Bowron, J.L. Finney, A.K. Soper, A structural investigation of solute–solute interactions in aqueous solutions of tertiary butanol, J. Phys. Chem. B 102 (1998) 3551–3563.
[13] D.T. Bowron, A.K. Soper, J.L. Finney, Temperature dependence of the structure of a 0.06 mole fraction tertiary butanol-water solution, J. Chem. Phys. 114 (2001) 6203–6219.
[14] D.T. Bowron, S. Diáz Moreno, The structure of a concentrated solution of tertiary butanol: water pockets and resulting perturbations, J. Chem. Phys. 117 (2002) 3753–3762.
[15] D.T. Bowron, J.L. Finney, Anion bridges drive salting out of a simple amphiphile from aqueous solution, Phys. Rev. Lett. 89 (2002) 215508-1–215508-4.
[16] S. Dixit, J. Crain, W.C.K. Poon, A.K. Soper, J.L. Finney, Molecular segregation observed in a concentrated alcohol-water solution, Nature 416 (2002) 829–832.
[17] S. Dixit, A.K. Soper, J.L. Finney, J. Crain, Water structure and solute association in dilute aqueous methanol, Europhys. Lett. 59 (2002) 377–383.
[18] J.L. Finney, A. Hallbrucker, I. Kohl, A.K. Soper, D.T. Bowron, Structures of high and low density amorphous ice by neutron diffraction, Phys. Rev. Lett. 88 (2002) 225503-1–225503-4.
[19] D.T. Bowron, A. Filipponi, M.A. Roberts, J.L. Finney, Hydrophobic hydration and the formation of a clathrate hydrate, Phys. Rev. Lett. 81 (1998) 4164–4167.
[20] R.D. Broadbent, G.W. Neilson, The interatomic structure of argon in water, J. Chem. Phys. 100 (1994) 7543–7547.
[21] J. Turner, A.K. Soper, J.L. Finney, Water structure in aqueous solutions of tetramethyl ammonium chloride, Mol. Phys. 77 (1992) 411–429.

[22] I.M. Svishchev, P.G. Kusalik, Structure in liquid water: a study of spatial distribution functions, J. Chem. Phys. 99 (1993) 3049–3058.
[23] F. Franks, J.E. Desnoyers, in: F. Franks (Ed.), Water Science Reviews, 1, Cambridge University Press, Cambridge, 1985, p. 171.
[24] J.N. Murrell, A.D. Jenkins, Properties of Liquids and Solutions, John Wiley, 1994.
[25] L.R. Pratt, D. Chandler, Theory of the hydrophobic effect, J. Chem. Phys. 67 (1977) 3683–3704.
[26] F. Franks, D.J.G. Ives, The structural properties of alcohol–water mixtures, Quar. Rev. 20 (1966) 1–45.
[27] A. Marmur, Dissolution and self-assembly: the solvophobic/hydrophobic effect, J. Amer. Chem. Soc. 122 (2000) 2120–2121.
[28] G. Palinkas, A. Hawlicka, K. Heinzinger, Molecular-dynamics simulations of water–methanol mixtures, Chem. Phys. 158 (1991) 65–76.
[29] K. Iwasaki, T. Fujiyama, Light-scattering study of clathrate hydrate formation in binary mixtures of *tert*-butyl alcohol and water, J. Phys. Chem. 81 (1977) 1908–1912.
[30] K. Iwasaki, T. Fujiyama, Light-scattering study of clathrate hydrate formation in binary mixtures of *tert*-butyl alcohol and water. 2. temperature effect, J. Phys. Chem. 83 (1979) 463–468.
[31] K. Nishikawa, H. Hayashi, T. Iijima, Temperature dependence of the concentration fluctuation, the Kirkwood-Buff parameters, and the correlation length of *tert*-butyl alcohol and water mixtures studied by small-angle x-ray scattering, J. Phys. Chem. 93 (1989) 6559–6565.
[32] T. Creighton, Proteins, Freeman, New York, 1993.
[33] P.L. Privalov, S.J. Gill, Stability of protein structure and hydrophobic interaction, Adv. Protein Chem. 39 (1988) 191–234.
[34] P.L. Privalov, N.N. Khechinashvili, Thermodynamic approach to the problem of stabilization of globular protein structure. A calorimetric study, J. Mol. Biol. 86 (1974) 665–684.
[35] R.M. Daniel, M. Dynes, H.H. Petach, The denaturation and degradation of stable enzymes at high temperatures, Biochem. J. 317 (1996) 1–11.
[36] D.A. Armitage, M.J. Blandamer, K.W. Morcom, N.C. Treloar, Partial molar volumes and maximum density effects in alcohol-water mixtures, Nature 219 (1968) 718–720.
[37] N.T. Skipper, Computer simulation of methane-water solutions, evidence for a temperature-dependent hydrophobic attraction, Chem. Phys. Lett. 207 (1993) 424–429.